Final Progress Report for Research Projects Funded by Health Research Grants

Instructions: Please complete all of the items as instructed. Do not delete instructions. Do not leave any items blank; responses must be provided for all items. If your response to an item is "None", please specify "None" as your response. "Not applicable" is not an acceptable response for any of the items. There is no limit to the length of your response to any question. Responses should be single-spaced, no smaller than 12-point type. The report **must be completed using MS Word**. Submitted reports must be Word documents; they should not be converted to pdf format. Questions? Contact Health Research Program staff at 717-783-2548.

1. **Grantee Institution:** Magee-Womens Research Institute and Foundation

2. **Reporting Period (start and end date of grant award period):** 1/1/2012-12/31/2012

3. **Grant Contact Person (First Name, M.I., Last Name, Degrees):** Cheryl Richards, MBA

4. **Grant Contact Person's Telephone Number:** (412) 641-8932

5. **Grant SAP Number:** 4100057668

6. **Project Number and Title of Research Project:** Project 3: Targeting Women's Cancer Cells with Novel Cell Cycle Inhibitors Blocking Centrosome Clustering

7. **Start and End Date of Research Project:** 1/1/2012-12/31/2012

8. **Name of Principal Investigator for the Research Project:** Calvin R. Simerly, Ph.D.

9. **Research Project Expenses**.

   9(A) Please provide the total amount of health research grant funds spent on this project for the entire duration of the grant, including indirect costs and any interest earned that was spent:

   $ $198,758.22

   9(B) Provide the last names (include first initial if multiple individuals with the same last name are listed) of **all** persons who worked on this research project and were supported with health research funds. Include position titles (Principal Investigator, Graduate Assistant, Post-doctoral Fellow, etc.), percent of effort on project and total health research funds expended for the position. For multiple year projects, if percent of effort varied from year to year, report in the % of Effort column the effort by year 1, 2, 3, etc. of the project (x% Yr 1; z% Yr 2-3).

Last Name	Position Title	% of Effort on Project	Cost
Simerly	PI/Research Associate Professor	28%	$40,877.40
Schatten	Professor & Vice Chair	12%	$24,964.00
Hartnett	Senior Research Associate	25%	$15,744.80
McFarland	Research Associate	10%	$4,267.62

9(C) Provide the names of **all** persons who worked on this research project, but who *were not* supported with health research funds. Include position titles (Research Assistant, Administrative Assistant, etc.) and percent of effort on project. For multiple year projects, if percent of effort varied from year to year, report in the % of Effort column the effort by year 1, 2, 3, etc. of the project (x% Yr 1; z% Yr 2-3).

Last Name	Position Title	% of Effort on Project
None		

9(D) Provide a list of **all** scientific equipment purchased as part of this research grant, a short description of the value (benefit) derived by the institution from this equipment, and the cost of the equipment.

Type of Scientific Equipment	Value Derived	Cost
None		

10. Co-funding of Research Project during Health Research Grant Award Period. Did this research project receive funding from any other source during the project period when it was supported by the health research grant?

Yes_____ No_____X____

If yes, please indicate the source and amount of other funds:

11. Leveraging of Additional Funds

11(A) As a result of the health research funds provided for this research project, were you able to apply for and/or obtain funding from other sources to continue or expand the research?

Yes_____ No __X____

If yes, please list the applications submitted (column A), the funding agency (National Institutes of Health—NIH, or other source in column B), the month and year when the application was submitted (column C), and the amount of funds requested (column D). If you have received a notice that the grant will be funded, please indicate the amount of funds to be awarded (column E). If the grant was not funded, insert “not funded” in column E.

Do not include funding from your own institution or from CURE (tobacco settlement funds). Do not include grants submitted prior to the start date of the grant as shown in Question 2. If you list grants submitted within 1-6 months of the start date of this grant, add a statement below the table indicating how the data/results from this project were used to secure that grant.

A. Title of research project on grant application	B. Funding agency (check those that apply)	C. Month and Year Submitted	D. Amount of funds requested:	E. Amount of funds to be awarded:
None	☐ NIH ☐ Other federal (specify:_____) ☐ Nonfederal source (specify:_)		$	$

11(B) Are you planning to apply for additional funding in the future to continue or expand the research?

Yes____X_____ No_____

If yes, please describe your plans:

We are seeking NIH Research sponsorship.

12. Future of Research Project. What are the future plans for this research project?

We are seeking NIH Research sponsorship for our findings that molecular motors and centrosome organizers are unique targets for cancer therapeutics.

13. New Investigator Training and Development. Did students participate in project supported internships or graduate or post-graduate training for at least one semester or one summer?

Yes_____ No_____X_____

If yes, how many students? Please specify in the tables below:

	Undergraduate	Masters	Pre-doc	Post-doc
Male				
Female				
Unknown				
Total				

	Undergraduate	Masters	Pre-doc	Post-doc
Hispanic				
Non-Hispanic				
Unknown				
Total				

	Undergraduate	Masters	Pre-doc	Post-doc
White				
Black				
Asian				
Other				
Unknown				
Total				

14. Recruitment of Out-of–State Researchers. Did you bring researchers into Pennsylvania to carry out this research project?

Yes_____ No_____X_____

If yes, please list the name and degree of each researcher and his/her previous affiliation:

15. Impact on Research Capacity and Quality. Did the health research project enhance the quality and/or capacity of research at your institution?

Yes____X_____ No_____

If yes, describe how improvements in infrastructure, the addition of new investigators, and other resources have led to more and better research.

This sponsorship was invaluable for the Pennsylvania investigators to develop new sophisticated dynamic approaches for investigating microtubule-mediated motility in living cancer cells using time-lapse video microscopy, and has been instrumental in recruiting new National Cancer Institute resources to programs here. Furthermore, this sponsorship has been leveraged to recruit new collaborations to the Commonwealth and we are optimistic that further dividends will accrue.

16. Collaboration, business and community involvement.

16(A) Did the health research funds lead to collaboration with research partners outside of your institution (e.g., entire university, entire hospital system)?

Yes_____ No___X_____

If yes, please describe the collaborations:

16(B) Did the research project result in commercial development of any research products?

Yes_____ No___X_____

If yes, please describe commercial development activities that resulted from the research project:

16(C) Did the research lead to new involvement with the community?

Yes_____ No___X____

If yes, please describe involvement with community groups that resulted from the research project:

17. Progress in Achieving Research Goals, Objectives and Aims.

List the project goals, objectives and specific aims (as contained in the grant agreement). Summarize the progress made in achieving these goals, objectives and aims for the period that the project was funded (i.e., from project start date through end date). Indicate whether or not each goal/objective/aim was achieved; if something was not achieved, note the reasons why. Describe the methods used. If changes were made to the research goals/objectives/aims, methods, design or timeline since the original grant application was submitted, please describe the changes. Provide detailed results of the project. Include evidence of the data that was generated and analyzed, and provide tables, graphs, and figures of the data. List published abstracts, poster presentations and scientific meeting presentations at the end of the summary of progress; peer-reviewed publications should be listed under item 20.

This response should be a DETAILED report of the methods and findings. It is not sufficient to state that the work was completed. Insufficient information may result in an unfavorable performance review, which may jeopardize future funding. If research findings are pending publication you must still include enough detail for the expert peer reviewers to evaluate the progress during the course of the project.

Health research grants funded under the Tobacco Settlement Act will be evaluated via a performance review by an expert panel of researchers and clinicians who will assess project work using this Final Progress Report, all project Annual Reports and the project's strategic plan. After the final performance review of each project is complete, approximately 12-16 months after the end of the grant, this Final Progress Report, as well as the Final Performance Review Report containing the comments of the expert review panel, and the grantee's written response to the Final Performance Review Report, will be posted on the CURE Web site.

There is no limit to the length of your response. Responses must be single-spaced below, no smaller than 12-point type. If you cut and paste text from a publication, be sure symbols print properly, e.g., the Greek symbol for alpha (α) and beta (ß) should not print as boxes (□) and include the appropriate citation(s). DO NOT DELETE THESE INSTRUCTIONS.

Goals: The dividing of one cell into two requires the proper functioning of the mitotic spindle, which separates the chromosomes, and is organized by the cell's two centrosomes. Centrosome aberrations cause cancers and birth defects by inducing chromosome errors leading to aneuploidies after mitosis. Genomic instabilities correlate with the degree of centrosomal abnormalities. At mitosis, extra centrosomes increase spindle multipolarity, a hallmark of many cancers. Recently, some cancers have been found to cluster supernumerary centrosomes at a bipolar spindle, avoiding multipolarity and activation of the internal cell death program while preserving reasonable genomic stability after cell division. Here, dynamic confocal imaging with living markers for centrioles and microtubules is used to investigate cell cycle inhibitors' impact on centrosome clustering and multipolarity at mitosis in normal somatic and cancerous cells.

Objectives: Understanding the dynamics and molecular composition of the cell's spindle poles and centrosomes in normal and cancerous cells affords new targets for designing chemotherapeutic strategies in oncology. This may well translate into innovative cancer treatments, but is also of keen importance for understanding the basic biology of every cell during division. Understanding the molecular mechanism of increasing multipolarity in cancer cells without subsequent effects on normal somatic cells would permit new strategies for the treatment of malignancies. It may also afford a much richer understanding of the link between spindle multipolarity, aneuploidy, and malignancy transformation in humans and, perhaps, give insights into innovative approaches for personalized treatment of cancers.

Aims:

AIM 1. Is centrosome clustering dependent on the expression patterns of molecular motors (dynein, HSET, dynactin) and NuMA at the spindle poles in cancerous and noncancerous cancer cells?

AIM 2. How does the Cdk1 inhibitor RO3306 affect cell cycle progression and centrosome duplication in cancerous versus noncancerous cells and expression of microtubule minus end molecular motors?

AIM 3. Using dynamic confocal imaging with a living marker for centrioles or microtubules, does Cdk1 inhibitor RO3306 prevent centrosome clustering and/or increase spindle multipolarity at metaphase in cancer cells following drug rescue?

AIM 4. Does the PARP inhibitor PJ-34 block cell cycle progression and centrosome clustering at the metaphase spindle poles with or without RO3306 exposure in cancer versus noncancerous cells?

Research Progress.

AIM 1. Is centrosome clustering dependent on the expression patterns of molecular motors (dynein, HSET, dynactin) and NuMA at the spindle poles in cancerous and noncancerous cancer cells?

Expression of the minus end motor proteins dynein and dynactin1, as well as the microtubule-binding nuclear mitotic apparatus (NuMA) protein, in methanol-fixed metaphase spindles of WI-38, NCI H292, and MCF7 cells is summarized in Figure 1. Cells attached to coverslips were fixed for 5 min in cold (-20ºC) absolute methanol for 10 min, rehydrated in phosphate-buffered saline with 0.25% Triton X-100 detergent (PBS-TX), and primary antibodies applied overnight at 4ºC (rabbit anti-dynein 1:100; rabbit anti-dynactin 1:100 or rabbit anti-NuMA 1:300; rat YOL 1/34 antitubulin antibody 1:200; mouse acetylated α-tubulin antibody 1:100). After rinsing off primary antibodies with PBS- TX, a cocktail of secondary antibodies, diluted 1:200, was applied overnight at 4ºC to detect primary antibodies. After a final rinse in PBS-TX, the DNA was detected using Hoechst 33342 at 10 µg/ml for 5 minutes before mounting stained coverslips in an antifade solution and sealing with nail varnish. Fixed cells were observed using a Nikon A1 laser scanning confocal microscope and selected images archived using Elements software. From the analysis of the staining patterns, dynein was greatly reduced in centrosomes and spindle poles in both NCI H292 and MCF7 cancer cell lines relative to WI-38 control fibroblast metaphase spindles (Figs. 1A, 1D, and 1G). Conversely, dynactin 1 was not reduced in cancer cell metaphase spindles (Figs. 1B, 1E, and 1H). We did not detect overexpression of NuMA in the spindle pole microtubules of either NCI H292 or MCF7 cancer cell lines relative to WI-38 control fibroblast cells (Figs 1C, 1F and1I:).

We explored NuMA staining patterns in noncancerous and cancer cells following nocodazole or paclitaxel microtubule inhibitor treatment. Cells attached to coverslips were exposed to either 10 µM nocodazole or 10 µM paclitaxel for 1 hr prior to methanol fixation as described above. In some cases, rescue experiments were performed by rinsing away the drug and permitting recovery in normal culture medium for 5 min prior to methanol fixation. Compared to control cells (Fig. 2A, 2D, 2G), 10 µM of nocodazole disassembled spindle microtubules in WI-38 (Fig. 2B), NCI H292 (Fig. 2E) and MCF7 (Fig. 2H) cells, with the loss of NuMA (Figs 2B, 2E, and 2H), although some NuMA detection at centrosome pairs (Fig. 2E) or filament-like structures in the cytoplasm (Fig. 2H) was observed. Also, rescue experiments from nocodazole showed reassembly of microtubules and NuMA association with developing spindle poles (Fig. 2B). Analysis of 10 µM paclitaxel drug treatment for 1 hr showed greatly enhanced astral microtubules in mitotic cells of all three cell lines (Figs. 2C, 2F, 2I), with a significant increase in NuMA detection (Figs. 2C, 2F, and 2I). Interestingly, increasing 10 µM paclitaxel drug treatment to 24 hrs significantly decreased dynein 70.1 detection at the centrosomes in WI-38 lung fibroblasts (Fig. 3A) and both cancer cell lines (Fig. 2C, 2E, and 3A).

Dramatic alteration of dynactin1 at the centrosomes was also observed in all three cell lines tested (Fig. 3B, 3D, 3F). NuMA remained visible in interphase nuclei after paclitaxel treatment (data not shown). Rescue experiments showed the reassembly of microtubules from centrosomes and NuMA association with these microtubules in control WI-38 cells, but not from NCI H292

and MCF7 cancer cells, after 5 minutes, suggesting cancer cells are slower to reassemble microtubules than control fibroblasts (data not shown).

Finally, we tested the patterns of molecular motors and NuMA in WI-38, NCI H292, and MCF7 cancer cells following exposure to the Cdk-1 inhibitor RO3306 (Figure 4). Cell lines were grown on coverslips in the presence of 20 μM of RO3306i/10 μM verapamil (a third-generation p-glycoprotein inhibitor used to block multidrug resistance in cancer cells) for 72 hrs before fixation as described above. In WI-38 control cells, dynein 70.1 and dynactin1 were retained at the spindle pole centrosomes (Figs. 4A, 4D) while NuMA was tightly associated with the bipolar spindle poles (Fig. 4G). In NCI H292 lung carcinoma cells, dynein 70.1 was weakly visible at multiple spindle poles (Fig 4B), dynactin1 was present at each spindle centrosome (Fig. 4E), and NuMA remained associated with spindle poles that retained an identifiable centriole (Fig. 4H). In MCF7 breast cancer cells, dynein 70.1 was largely absent at the spindle centrosomes (Fig. 4C), dynactin1 retained at centriole-containing spindle poles (Fig. 4F), and NuMA retained at spindle pole microtubules (Fig. 4I). Collectively, these data indicate that both NCI H292 and MCF7 cancer cells are deficient in dynein heavy chain protein at their spindle poles and demonstrate slower microtubule dynamics than the WI-38 lung fibroblast line.

Although dynein, dynactin, and NuMA are reportedly present as a tri-molecular complex at mitotic spindle poles, and the loss of one of these proteins may be overcome by redundant activity of the other complex members, these observations hint at molecular motor importance in the mechanism of bipolar spindle pole organization and, perhaps, in centrosome clustering.

We successfully expressed pEGFP-C1-NuMA vector in all three cell lines and showed these cells to be viable by performing time-lapse video microscopy (TLVM) of mitosis through cell division (Figs. 5, 6, and 7). Cells were seeded onto glass coverslips and grown to approximately 70% confluence before transfecting with 2 μg/ml pEGFP-C1-NuMA plasmid using Lipofectamine 2000 for 4 hrs. Analysis showed all three cell lines successfully transfected with eGFP-C1-NuMA. After fixation in 1% formaldehyde for 10 min, we confirmed eGFP-C1-NuMA expression in interphase nuclei of WI-38 and NCI H292 lung carcinoma cells at an efficiency of more than 75% of the cells (Figs. 5A and C). By live-cell imaging of eGFP-C1-NuMA (Fig. 6), we could detect both interphase (Fig. 6A-B) and mitotic cells (Fig. 6C-F) in all of our cell lines. We also showed that cells expressing GFP-NuMA were not impaired in growth and cell cycling.

Cells expressing eGFP-C1- NuMA were plated onto glass-bottom 35 mm sterile dishes, and TLVM was performed on a Nikon inverted Ti Eclipse microscope using a Tokai stage incubator to maintain 37ºC and 5% CO_2 throughout imaging. Mitotic cells were identified by eGFP-C1-NuMA at the spindle poles, and z- stack images were collected every 2 min using attenuated fluorescent exposure and Oxyrase in phenol-red free medium to reduce photo bleaching during image collection. From 7 TLVM, we observed normal mitotic progression with NuMA reorganization from the spindle poles to daughter nuclei during their reassembly at the end of cell division (Fig. 7). We also examined eGFP-C1-NuMA expression in cancer cells following Cdk-1 inhibition by RO3306i (Fig. 8). Mitotic cells appeared to overexpress NuMA after RO3306 treatment, but most of these cells did not undergo mitotic exit or complete cell division following drug recovery and TLVM.

Taken together, these findings show that cancer cells can effectively express eGFP-C1-NuMA without affecting cell viability. Use of these transduced cancer cell lines in analyzing bipolar spindle assembly, in NuMA translocation from nuclei to spindle poles, and in centrosome behavior during mitosis, is an exciting prospect for the future.

We investigated whether the knockdown of endogenous NuMA protein with a shRNA NuMA probe (Santa Cruz Biotechnology, Inc, Santa Cruz, CA) would increase spindle multipolarity and centrosome dispersion at the spindle poles in cancer cells. NCI H292 lung carcinoma cells and MCF7 breast cancer cells were plated in a T-25 flask for 24 hours to approximately 50% confluency. The cell medium was replaced with 5 ml of a 5 $\mu g\ ml^{-1}$ Polybrene before adding 20 μl of shRNA NuMA lentiviral particles to flasks for overnight incubation at 37°C in 5% CO_2. The following day, the cells were rinsed three times in normal culture media and incubated overnight. Cells expressing shRNA were passaged 1:3 to 1:5 for 48 hrs before selection of stably transduced cells using 10 $\mu g\ ml^{-1}$ puromycin dihydrocholoride over a 3–4 day period.

As shown in Figure 9A, Western blots of protein extracts of transduced shRNA NuMA cells showed measurable changes in endogenous NuMA in both NCI H292 cells (-31%) and MCF7 cells (-42%) relative to control cell line extracts. Attempts at increasing shRNA NuMA transduction were found to be detrimental to cell survivability. Immunocytochemistry (ICC) analysis did not show complete disruption of NuMA from spindle pole microtubules or the cell cortex (Fig. 9B). Spindle assembly was mostly bipolar, with normal centriolar organization and aligned chromosomes (Figs. 9B and 10).

We also explored whether combined shRNA NuMA knockdown with RO3306i with verapamil would impact spindle multipolarity and centrosome organization. Control NCI H292 cells treated with15μM RO3306/10 μM verapamil for 72 hrs demonstrated an increased percentage of cells expressing abnormal spindle poles, centriole amplification, and misaligned chromosomes (Fig. 9C). NuMA was observed in most spindle pole microtubules, with some reduction observed at extra supernumerary spindle poles (Figs. 9C and 10).

Likewise, shRNA NuMA NCI H292 cells treated with 15μM RO3306/10 μM verapamil for 72 hrs showed similar increases in multipolar spindles, centriole hyperamplification, abnormal NuMA at some poles, and misaligned chromosomes (Figs. 9D and 10).

We also performed TLVM imaging on shRNA knockdown, GFP-centrin-expressing NCI H292 lung carcinoma control or RO3306i cells (Fig. 11). We observed a few control mitotic shRNA NuMA knockdown, GFP centrin-tagged cells which appeared to undergo normal division with appropriate centriole inheritance in daughter cells. Interestingly, NCI H292 cells treated for 72 hrs with RO3306i appeared to overduplicate centrioles, some of which may have clustered at one of the spindle poles. Z-series TLVM taken at 2-minute intervals for 1 hour showed this cell with multiple centrioles still divided correctly into two daughter cells. Taken together, Cdk-1 inhibition by RO3306/verapamil initiates a significant increase in spindle multipolarity, centriole amplification, and DNA misalignment in cancer cells, but a minority of these cells appear to handle hyperamplification of centrioles by clustering at spindle poles prior to cell division. Knockdown of endogenous NuMA by the lentiviral shRNA NuMA at amounts sufficient to

ensure cell survival was probably not sufficient to drop NuMA below the critical thresholds necessary to impact microtubule minus end organization in spindle poles.

AIM 2. How does the Cdk1 inhibitor RO3306 affect cell cycle progression and centrosome duplication in cancerous versus noncancerous cells and expression of microtubule minus end molecular motors?

We determined the effects of the Cdk1 inhibitor RO3306 on cell cycle progression and on bipolar spindle assembly, centrosome amplification, and chromosome alignment in NCI H292 and MCF7 cancer cell lines (Fig. 12). Cells were grown in the presence of 10 μM of RO3306 per 10 μM of verapamil for 72 hrs, followed by formaldehyde fixation and ICC analysis using antibodies to centrioles (Cep 135), microtubules, and DNA. A G2/M cell cycle arrest was not observed in either NCI H292 or MCF7 cells grown in the presence of RO3306i, although the incidence of normal bipolar spindle assembly was significantly reduced, with a significant increase in abnormal mitotic centrosome numbers and misaligned chromosomes at metaphase. Collectively, the data suggest that the Cdk1 inhibitor RO3306 does not arrest cell cycle progression but does uncouple the centrosome cycle from the DNA replication cycle, permitting centrosome amplification, multipolar spindle assembly, and chromosome congression defects.

We sought to understand more about cell cycle progression after RO3306i in our cancer cell lines. We explored the use of the live dynamic cell cycle marker probe G1S in all three cell lines. We added 2 μg of G1S plasmid and transduced cells with Lipofectamine 2000. After transfection and recovery for 24 hrs, live cell TLVM imaging was performed as previously described. Using this probe, we could determine G1- versus S-, G2-, and M-phase cells in culture (Fig 13), but the efficiency was low, and the fluorescein indicator interfered with our simultaneous imaging of GFP centrin-tagged cell lines. Thus, we examined whether Cdk-1 inhibition by RO3306 blocked cell cycle progression in cancer cells by examining bromodeoxyuridine (BrDU) incorporation at 48 or 72 hrs post drug application.

MCF7 cells were plated at 4×10^4 cells per well for 24 hrs before adding 10 μM of RO3306 per 10 μM of verapamil. About 16 hrs prior to fixation, 20 μM of BrDU labeling reagent was added to the culture. After fixation according to the manufacturer's instructions, BrDU was detected with a mouse anti-BrDU antibody and the number of BrDU-positive cells counted in 5–8 fields. We determined that RO3306i reduced the number of MCF7 cells progressing through S phase of the cell cycle by 75% at 48 hrs and 70% by 72 hrs post inhibitor treatment compared to control cells exposed to 10 μM verapamil alone (Fig. 14). Thus, RO3306i may impact DNA replication onset, with cells arresting earlier in the cell cycle than the predicted G2/S phase as reported for Chinese hamster ovary cells.

AIM 3. Using dynamic confocal imaging with a living marker for centrioles or microtubules, does Cdk1 inhibitor RO3306 prevent centrosome clustering and/or increase spindle multipolarity at metaphase in cancer cells following drug rescue?

We prepared stable GFP centrin-expressing WI-38, NCI H292, and MCF7 cell lines using pEGFP-CETN2 construct (donated generously by Dr. Jeffrey Salisbury, Mayo Clinic, MN) following the production of lentiviral particles using ViraPower Lentiviral Packaging Mix (Life

Technologies, Carlsbad, CA). All cell lines were grown in T-25 cell culture flasks to 30–40% confluency before applying a solution of 60 µLs of concentrated GFP centrin lentivirus and 6 mg/mL of Polybrene (Sigma) in complete culture media. Virus-exposed cells were incubated overnight at 37°C before expression of GFP centrin was determined by inverted fluorescent microscopy. Cell lines were determined to be stably transduced on the basis of a greater than 75% GFP centrin detection following numerous cell passages, as well as following cryopreservation and thawing for reconstituting cell lines *in vitro*. As summarized in Table 1, we imaged 74 NCI H292 or MCF7 cancer cells by TLVM after stably transducing with the pEGFP-CETN2 (GFP-centrin) construct.

Control WI-38 lung fibroblast cells were inefficient at transduction with the GFP centrin construct, with only one of four attempts successful at four times the concentration of lentiviral particles which produced success in the cancer lines. However, the WI-38 cells exposed to the highest concentration of GFP centrin construct did not propagate effectively *in vitro*, and mitotic cells were rarely observed in culture. Exposure of successfully transduced GFP centrin WI-38 cells to 12 µM RO3306 per 10 µM verapamil did show hyperamplification of centrioles in a few interphase cells, although most displayed normal duplicated centrioles after RO3306i (Fig. 15).

For GFP centrin-tagged NCI H292 lung carcinoma cells, we imaged 19 cells exposed to 10 µM of verapamil only (controls) and another 18 cells after RO3306i (Table 1). Control interphase NCI H292 cells rarely entered mitosis during imaging, perhaps owing to cumulative photodamage over long imaging periods (> 18 hrs). However, extensive centriole movement within the cytoplasm was observed during interphase, confirming previous reports that centrioles in cancer cells are not restricted to just nuclear association (data not shown). Additionally, all 10 control mitotic NCI H292 cells completed normal cell division within 1–2 hrs post imaging (Fig. 18A-F). As observed in control interphase NCI H292 cells, lung carcinoma cells exposed for 48 hrs to RO3306i did not enter mitosis often. Figure 16 analyzes one NCI H292 cell expressing GFP centrin and exposed to 10 µM RO3306 that demonstrated amplified centrosomes (Fig. 16A) which separated prior to entrance into mitosis (Fig 16B-E) and, followed over the next 2 hours, showed nuclear envelope breakdown, bipolar spindle assembly, and cell division from 1→2 cells despite multiple centrioles (Fig. 16F-L). TLVM analysis suggested that the extra centrioles did not "cluster" at the spindle poles at metaphase (Fig. 16 F), although only two centrioles were observed in this cell during anaphase and telophase transitions (Fig. 16G and H). After cell division, multiple centrioles were observed in the daughter cells (Fig. 16, I-L).

We also imaged an additional six mitotic GFP centrin-tagged NCI H292 cells after RO3306i, with 50% undergoing cell division during imaging (Table 1). As shown in Figure 17, Cdk-1 inhibition with 10 µM RO3306/10 µM verapamil for 72 hr produced cells with amplified centriole numbers that initially appeared clustered at the assembling spindle poles (Fig. 17A). As mitosis ensues, a single centriole appears to migrate away from the cluster to form a third distinct spindle pole by late anaphase (Fig. 17B-F). Division initially appears to be 1→3 daughter cells, each with a distinct set of centrioles (Fig. 17G), but two blastomeres actually coalesce to form two daughter cells at the end of cell division (Fig. 17H). Increasing RO3306i to 15 µM RO3306/10 µM verapamil for 72 hr increased NCI H292 cell percentages with amplified centrioles that could enter mitosis, but most cells could not complete mitotic progression including chromosome segregation and cell division (Fig. 18G-L).

For GFP centrin-tagged MCF7 breast cancer cells, we imaged nine control cells after 10 μM verapamil or 1 μM Tariquidar, a third generation p-glycoprotein inhibitor that prevents multi-drug resistancy in cancer cells, and 23 MCF7 cells after RO3306i. For control MCF7 cells, 63% completed normal cytokinesis (Table 1) while cells treated with RO3306i were significantly prevented from entering mitosis (7%) or completing normal cell division (17%). GFP centrin-tagged MCF7 cells exposed to 10 μM RO3306/10 μM verapamil for 48 hrs showed many cells with hyperamplification of centrioles at interphase (Figs. 19A and 20A). At mitosis, some mitotic MCF7 cells assembled spindles in the presence of multiple centrioles, some of which initially appeared to cluster at the poles (Fig. 19B-E). However, this process could take more than 10 hrs to accomplish, (Fig. 19F) and cytokinesis failed after initial cleavage furrow formation (Fig. 19F-H). Other MCF7 cells treated with RO3306i showed centrioles that migrated away from the spindle poles into the cytoplasm with the eventual collapse of the bipolar spindle without cytokinesis ensuing (Fig. 20).

Collectively, the TLVM data suggest that cancer cells have multiple methods for assembling bipolar spindles and completing cytokinesis in the presence of hyperamplified centrioles, including centriole spindle dissociation after spindle assembly and daughter cell fusion at the end of cytokinesis. Overall, the mechanism of "clustering" extra centrioles might be a very rare event. We have speculated that the rare cells that do cluster extra centrioles to avoid apoptosis are "specialized" cells in the sense that they may represent robust progenitors which might convey unique advantages to these cells for propagating tumors.

AIM 4. Does the PARP inhibitor PJ-34 block cell cycle progression and centrosome clustering at the metaphase spindle poles with or without RO3306 exposure in cancer versus noncancerous cells? We tested the effects of the poly (ADP-ribose) polymerase (PARP) inhibitor PJ-34 (N-(6-oxo-5,6-dihydro-phenanthridin-2-yl)-N,N-dimethyl-acetamide) on bipolar spindle assembly and centrosome amplification in our cancerous and noncancerous cell lines. Recent reports have shown that certain cancer cells carrying supernumerary centrosomes are destroyed by PARP inhibitors like PJ-34 which act as 'de-clustering' centrosome agents that increases cell apoptosis. Initially, we incubated WI-38, NCI H292, and MCF7 cells in 10μM PJ-34 for 24, 48 and 72 hrs and fixed samples in 2% formaldehyde for immunostaining with antibodies to Cep 135 (centrosomes), microtubules and DNA as described in Aim 1. Under these conditions, no significant differences between WI-38 lung fibroblast cells, NCI H292 lung carcinoma or MCF7 breast cancer cells was observed for the percentage of cells that successfully assembled a bipolar spindle or showed hyperamplified centrosomes (after drug treatment) (Fig. 21). ICC analysis of 10μM PJ-34 noncancerous control cells showed the majority of cells having normal bipolar spindles with appropriate centriole numbers and position as well as aligned metaphase chromosomes (Fig. 21A-B). By contrast, PJ-34 treated cancer cells showed some typical multipolar spindles with four centrosomes and misaligned chromosomes (Fig. 21E-F), although no differences were detected between drug and control DMSO vehicle treated samples. In some images, centrosome 'clustering' was evident since metaphase spindles formed with multiple centrosomes at the bipolar spindle poles (Fig. 21C-D).

By raising the concentration of PJ-34 to 20 μM and co-incubating cells with 1 μM Tariquidar, however, we demonstrated a dramatic effect on the mitotic index rate in NCI H292 and MCF7 cancer cells (Fig. 21: bottom graph). We showed a 136-fold decrease in the number of total

mitotic cells in NCI H292 treated with PJ-34/Tariquidar compared to Tariquidar only control cells and a similar 86-fold reduction of mitotic MCF7 treated with PJ-34/Tariquidar compared to paired control cells. ICC analysis of control mitotic cancer cell lines demonstrated typical multipolar spindles (Fig. 21A and C, lower panel: red, microtubules) with amplified centrioles (Fig 21A and C: green, arrowheads, Cep135 centrioles) and poorly aligned chromosomes (Fig. 21A and C: blue, DNA). Conversely, cancer cells treated with 20 μM PJ-34/1 μM Tariquidar for 72 hours showed only bipolar spindles (Fig. 21B and D: red, microtubules) with normal centriole numbers and position at the poles (Fig. 21B and D: green, arrowheads, Cep 135 centrioles), although some cells displayed misaligned chromosomes (Fig. 21D: blue, DNA). Taken together, we conclude that PJ-34 does not prevent cell cycle progression in cancer cell lines but greatly diminishes the incidence of mitotic cells and particularly the presence of multipolar spindles classically identified in cancer cells. We speculate that PJ-34 may actually <u>increase</u> multipolar spindles early, with the consequence of increasing programmed cell death that eliminates abnormal cancer cells carrying amplified centrioles. By 72 hrs post drug treatment, mitotic cell numbers are greatly diminished and only bipolar spindles with correctly positioned centrioles at their poles are able to avoid activation of programmed cell death and apoptosis. Inducing amplification of centrioles with the Cdk-1 inhibitor RO3306 followed by treatment with PJ-34 is predicted to vastly diminish abnormal mitotic cancer cells in vitro and may represent a novel cancer therapy for future testing.

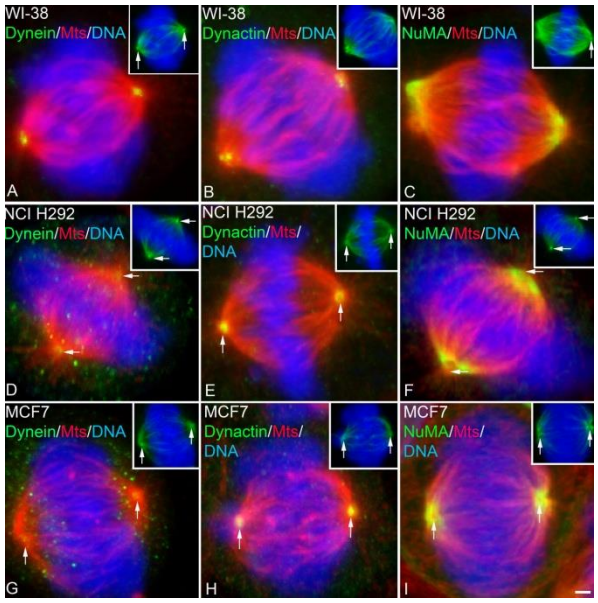

Figure 1. Detection of dynein, dynactin 1, and NuMA in noncancerous and cancer cell lines. A–C: metaphase spindles in WI-38 lung fibroblasts. The molecular motors dynein (A: green) and dynactin1 (B: green) are strongly detected at the spindle pole centrosomes while the microtubule binding protein NuMA (C: green) labels the spindle pole microtubules (C: green). Insets: acetylated α-tubulin detects both centrosomes and spindle pole microtubules (green) in WI-38 cells. Blue: DNA. Red: microtubules. D–F: Metaphase spindles in the lung cancer line NCI H292. Dynein detection is significantly reduced at the spindle poles and centrosomes (D: green, arrows; red, microtubules; blue, DNA) compared to WI-38 cells, although both dynactin1 and NuMA are strongly observed at the centrosomes (E: green, arrows) and spindle pole microtubules (F: green, arrows), respectively. Insets: acetylated α-tubulin (green) and DNA in same spindles, showing centrosome detection (arrows) at metaphase. G–I: Metaphase spindles in MCF7 breast cancer cell line. Dynein detection is significantly reduced at the spindle poles in MCF7 cells (G: green, arrows) while both dynactin 1 (H: green, arrows) and NuMA (I: green, arrows) strongly detect centrosomes and spindle pole microtubules. Inset: acetylated α-tubulin labeling of centrosomes (green, arrows) and spindle pole microtubules. All images quadruple-labeled for dynein, dynactin, or NuMA (green); microtubules (red); DNA (blue); and acetylated α-tubulin (cy5 image, color assigned green). Bar= 1μm.

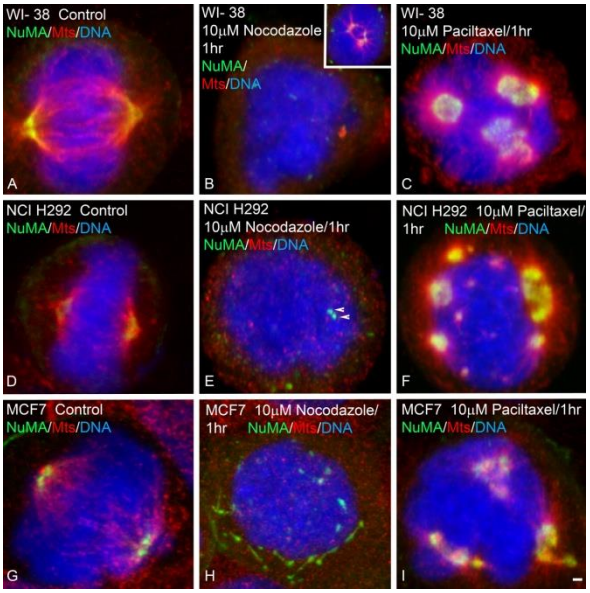

Figure 2. NuMA localization in mitotic WI-38 lung fibroblast, NCI H292 lung carcinoma, and MCF7 breast cancer cells following cytoskeleton inhibition with nocodazole and paclitaxel. A–C: WI-38 lung fibroblasts. A: Control metaphase WI-38 cell with NuMA localization at both spindle poles (green; red, microtubules; blue, DNA). B: Microtubule (Mt) disassembly with 10 μM nocodazole for 1 hr disrupts spindle Mts (red; blue, DNA), and NuMA is dispersed into the cytoplasm (green). B, Inset: Nocodazole-treated cell recovered for 5 min, showing Mt reassembly (red) and NuMA binding to developing spindle poles (green; blue, DNA). C: Microtubule augmentation with 10 μM paclitaxel for 1hr shows extensive Mt polymerization (red) and

NuMA binding (green; blue, DNA) from multiple sites. D–F: NCI H292 lung carcinoma cells. D: Metaphase cell (blue, DNA) with a bipolar spindle (red, microtubules) and NuMA at the spindle poles (green). E: Mt disassembly with 10 μM nocodazole for 1 hr shows complete disassembly of spindle Mts (red; blue, DNA) and NuMA detection only at pair of centrioles (green, arrowheads). F: 10 μM paclitaxel for 1 hr dramatically assembles microtubules (red) with a large increase in NuMA detection at each Mt aster (green; blue, DNA). G–I: MCF7 breast cancer cells. G: Control MCF7 metaphase cell (blue, DNA) showing bipolar spindle (red, microtubules) and NuMA at the spindle poles (green). H: MCF7 mitotic cell (blue, DNA) after 10 μM nocodazole for 1 hr shows complete disassembly of the spindle Mts (red) and small cables of NuMA (green) in the cytoplasm. I: MCF7 mitotic cell (blue, DNA) after 10 μM paclitaxel for 1 hr. Note multiple Mt aster formation (red) and enhanced NuMA at each aster (green). All images triple-labeled for NuMA (green), microtubules (red), and DNA (blue). Bar= 1μm.

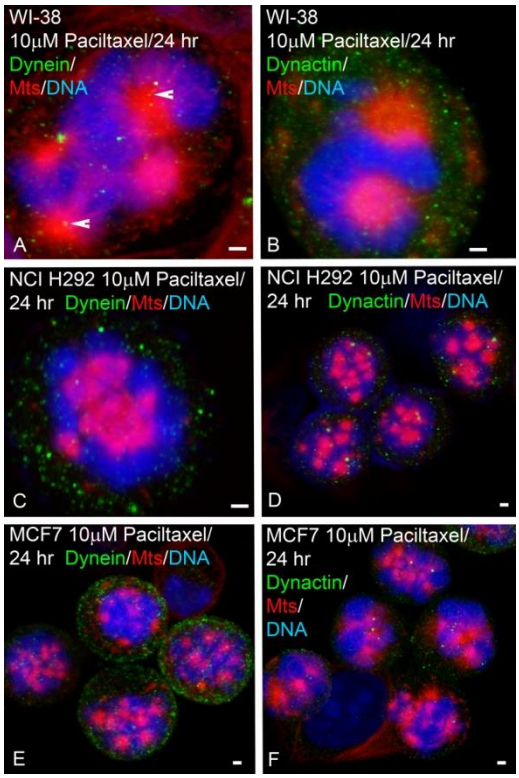

Figure 3. Alteration of dynein and dynactin1 in WI-38, NCI H292, and MCF7 cancer cells exposed to 10 μM paclitaxel for 24 hrs. A: Paclitaxel increases microtubule assembly from multiple asters (red, microtubules) in mitotic WI-38 cells (blue, DNA) with weak dynein 70.1 detection (green, arrowheads). B: Enhanced spindle poles (red, microtubules) in a mitotic WI-38 cell (blue, DNA) but without detection of dynactin1 at the centrosomes (green). C and E: Detection of dynein 70.1 in mitotic NCI H292 (C: blue, DNA) and MCF7 (E: blue, DNA) cancer cells. Microtuble assembly is enhanced by paclitaxel from multiple asters in both cancer cells (C and E: red, microtubules), but no dynein 70.1 is observed at the astral centers (C and E: green), although some cortical dynein is apparent in MCF7 cells (E: green). D and F: Detection of dynactin1 in NCI H292 (D) and MCF7 (F) cancer cells. Multiple microtubule asters are present in both cancer cells (D and F: red), but without detectable dynactin1 in the aster centers (D and F: green). Images are triple-labeled for dynein 70.1 or dynactin1 (green), microtubules (red) and DNA (blue). Bars= 1 μm.

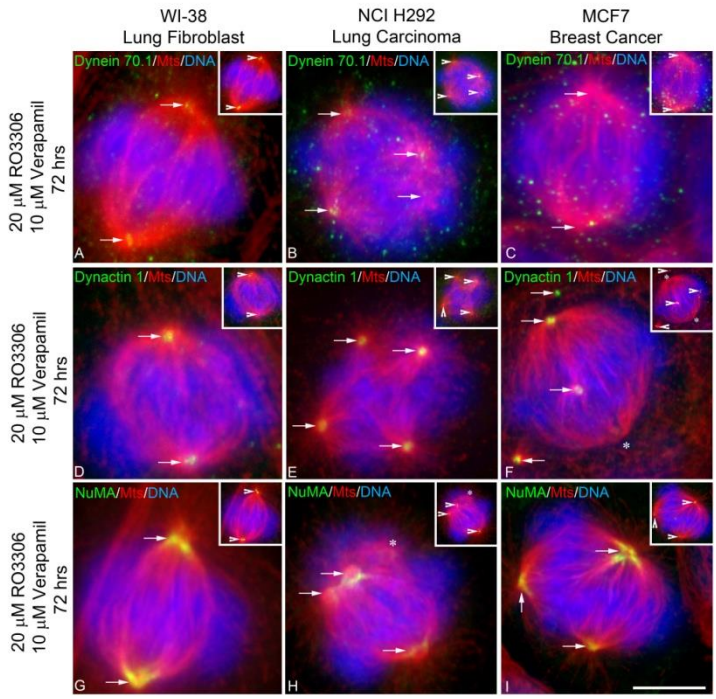

Figure 4. Detection of molecular motors and NuMA following Cdk-1 inhibition with 20 µM RO3306/10 µM verapamil for 72hrs in WI-38 lung fibroblast (A, D, G), NCI H292 lung carcinoma (B, E, H), and MCF7 cells (C, F, I). Dynein 70.1 remains strongly localized to the spindle pole centrosomes in WI-38 lung fibroblast cells (A: green, arrows; red, microtubules; blue, DNA) after Cdk1 inhibition by RO3306i. However, weaker detection of dynein 70.1 is observed in both NCI H292 (B: green, arrows) and MCF7 (C: green, arrows) cancer cells after Cdk-1 inhibition. Insets: Centrin (green), microtubules (red) and DNA (blue) of corresponding cells. D–F: Dynactin1 (D-F: green, arrows) is observed at all centrosomes (D-F: insets: green, arrowheads, centrin centrioles), but not all spindle poles (F: * denotes spindle pole without dyanctin1) after RO3306i. G–I: Likewise, NuMA (G-I: green, arrows) is detected at spindle poles (G-I: red, microtubules; blue, DNA) with centrioles (G-I: insets: green, centrin centrioles, arrowheads), but absent from spindle poles lacking centrioles (H: * denotes acentriolar spindle pole without NuMA or centrin detection). All insets: Corresponding images of centrin (green), microtubules (red) and DNA (blue). All images quadruple-labeled for dynein, dynactin1, or NuMA (green); microtubules (red); DNA (blue); and centrin 20H5 (Cy5 imaged, color assigned green). Bars= 5µm.

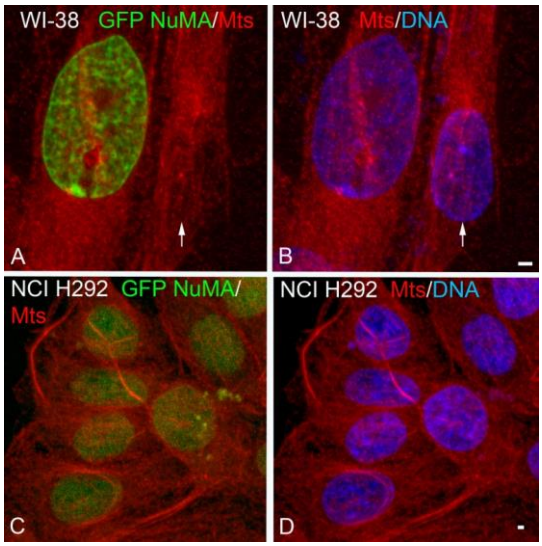

Figure 5. Detection of PeGFP-C1-NuMA expression in formaldehyde-fixed WI-38 and NCI H292 lung carcinoma cells. A–B: Transduced interphase WI-38 cells (B: red, microtubules; blue, DNA), with one cell expressing GFP-C1-NuMA in the nucleus (A: green; red, microtubules; arrow denotes unsuccessful transduced cell). C–D: Seven interphase NCI H292 lung carcinoma cells (D: red, microtubules; blue, DNA) expressing eGFP-C1-NuMA in the nucleus (C: green; red, microtubules). All images are double-labeled for microtubules (red) and DNA (blue). Bars= 1µm.

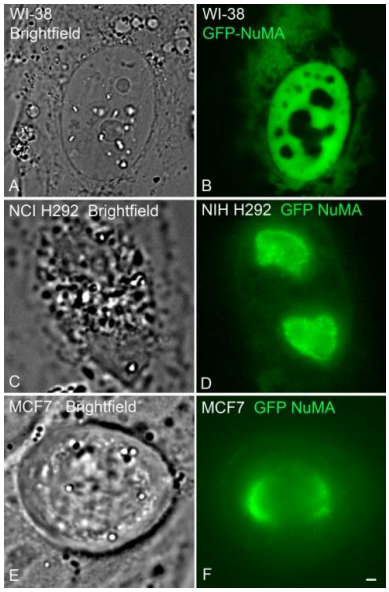

Figure 6. Live-cell imaging of eGFP-C1-NuMA in WI-38, NCI H292, and MCF7 cells. A–B: Interphase WI-38 lung fibroblast (A: bright field), showing intranuclear eGFP- C1-NuMA expression (B: green) 24 hrs post-transfection. C–D: NCI H292 cancer cell at late telophase (C: bright field), showing eGFP-C1-NuMA in reassembling daughter cell nuclei (D: green). E–F: Mitotic metaphase MCF7 breast cancer cell (E: bright field), showing eGFP- C1-NuMA at the mitotic spindle poles. All live-cell images were taken on an inverted Nikon Ti Eclipse microscope with a 100x Plan-Neofluar objective and captured with an Andor chilled, charge-coupled device camera using Elements software. Bar= 1µm.

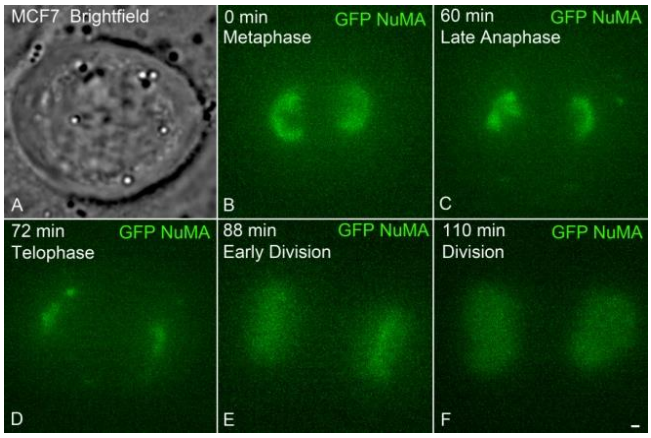

Figure 7. Time-lapse video microscopy of an MCF7 mitotic cell expressing eGFP-C1-NuMA. A: Bright field image. B–F: Live-cell imaging of eGFP-C1-NuMA expression (green) during mitosis, showing metaphase (B), anaphase (C), chromosome separation (D-E) and daughter cell formation (F) over 60 minutes of imaging. eGFP-C1-NuMA relocalizes from spindle microtubules to the daughter cell nuclei. Bar=1µm.

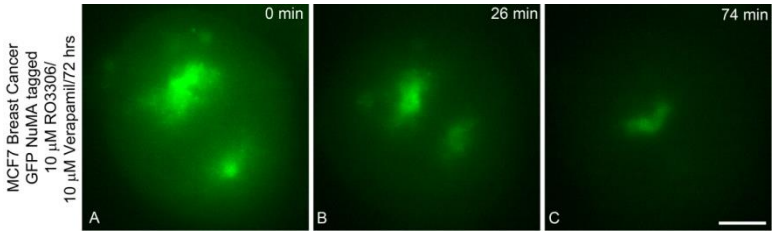

Figure 8. Time-lapse video microscopy of an MCF7 cell expressing eGFP-C1-NuMA and treated 72 hrs with 10 µM RO3306/10 µM verapamil. eGFP-C1-NuMA appears to be overexpressed in the cell at the start of imaging (A: green). However, this cell did not complete mitosis and, over the next 74 min, the eGFP-C1-NuMA began to diminish at the spindle poles as the spindle collapsed (B-C: green). Time: minutes post imaging. Bar=5 µm.

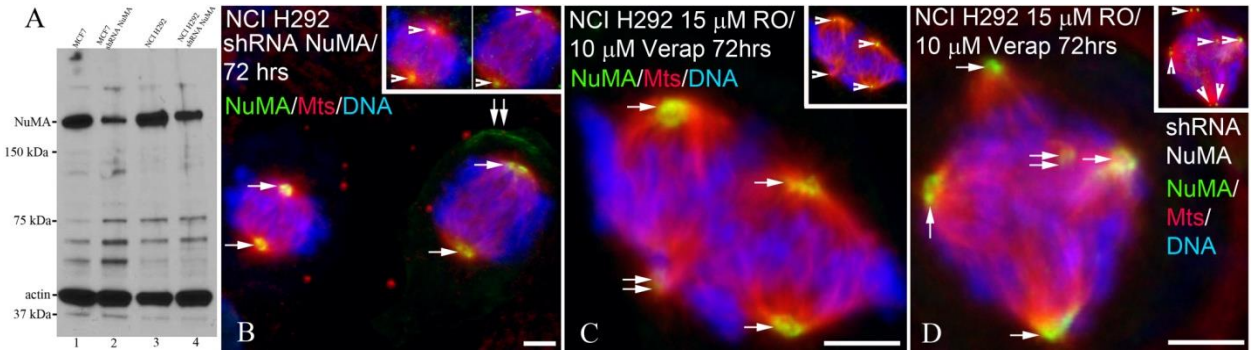

Figure 9. Knockdown of endogenous NuMA with shRNA in NCI H292 and MCF7 cancer cells. A: Western blot of MCF7 (Lanes 1 and 2) and NCI H292 (Lanes 3 and 4) protein extracts, showing 30–42% reduction of endogenous NuMA protein after shRNA transduction. B–D: Representative ICC figures of NCI H292 lung fibroblast cells after shRNA NuMA transduction and exposure to 15 μM RO3306/ 10 μM verapamil for 72 hrs. B: control mitotic NCI H292 cells (blue, DNA) after shRNA NuMA knockdown, showing typical bipolar spindle assembly (red, microtubules) and endogenous NuMA at the spindle poles (green, arrows; double arrows: NuMA at cell cortex). C: Tetrapolar NCI H292 cells after RO3306i for 72 hrs but without shRNA NuMA knockdown. NuMA (green, arrows) is strongly localized to three of four spindle poles (red, microtubules; blue, DNA). D: Mitotic NCI H292 cell after shRNA NuMA knockdown and treatment with RO3306i. This cell has five NuMA-localized spindle poles despite NuMA knockdown (green, arrows; red, microtubules) and misaligned DNA (blue). All insets: Centrin (green), microtubules (red), and DNA (blue). Bars= 5μm.

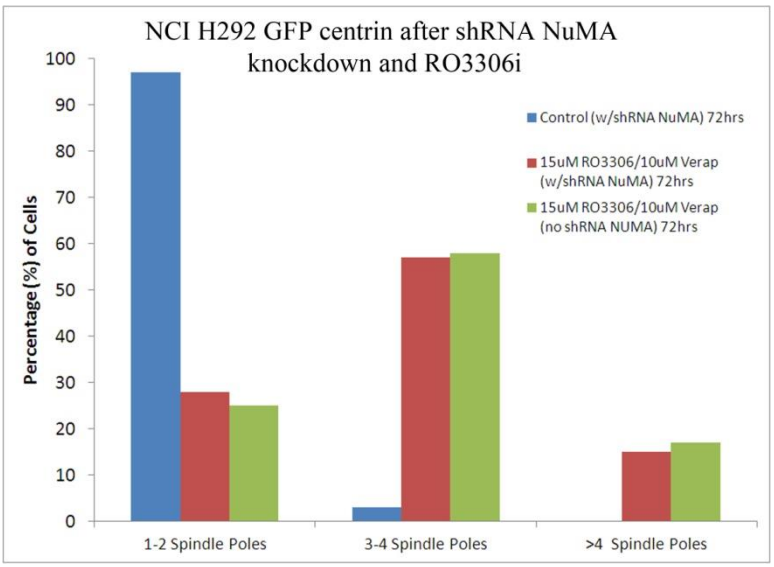

Figure 10. Graphic analysis of NCI H292 cells following shRNA NuMA knockdown and Cdk-1 inhibition by RO3306. Blue bars: Analysis of spindle pole numbers in control NCI H292 cells treated with shRNA NuMA. No increase in multipolar spindle assembly was evident. Green bars: NCI H292 cells treated with 15 μM RO3306/10 μM verapamil for 72 hrs demonstrated a significant increase in multipolar spindle assembly. Red bars: NCI H292 cells after shRNA NuMA and 15 μM RO3306/10 μM verapamil for 72 hrs showed increased multipolar mitotic spindles, but no significant difference from cells treated with RO3306i alone.

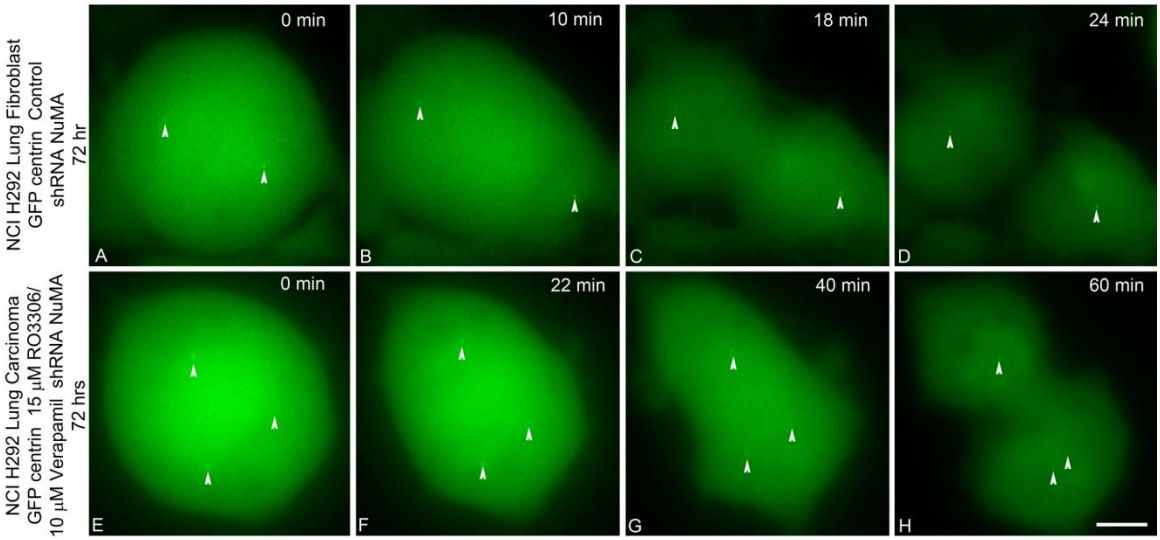

Figure 11. TLVM of NCI H292 lung carcinoma cell transduced with shRNA NuMA and exposed to 15 μM RO3306i/10 μM verapamil for 72hrs. A: control shRNA NuMA transduced bipolar metaphase cell treated with 10 μM verapamil only for 72hrs, showing GFP centrin-tagged centrioles at each spindle pole (green, arrowheads). B–D: Completion of mitosis and cell division over the next 24 min with the inheritance of a single centriole in each daughter cell (green, arrowheads). E–H: shRNA NuMA transduced multipolar mitotic cell derived by a 72-hr exposure to the Cdk-1 inhibitor 15 μM RO3306/10 μM verapamil. Imaging began 2.5 hrs post-drug recovery. At time=0, a tripolar spindle with three GFP centrin-tagged centrioles was observed (E: green, arrowheads). Over the next 60 min, this cell underwent chromosome segregation and cell division into two daughter cells despite the presence of multiple centrioles at one of the poles (F-H: green, GFP centrin, arrowheads). Bar= 5 μm.

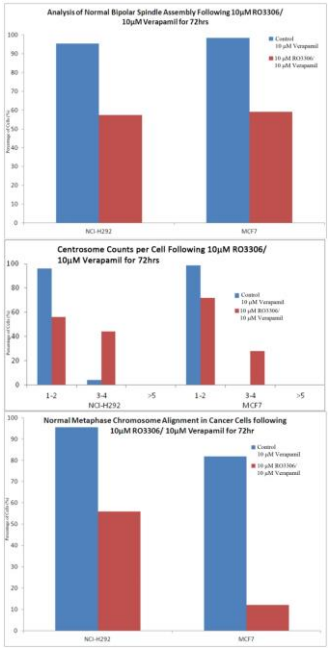

Figure 12. Bipolar spindle assembly, centrosome amplification, and normal chromosome alignment after Cdk-1 inhibition by 10 μM RO3306/10 μM verapamil for 72hrs on NCI H292 and MCF7 cancer cells. Top graph: The blue bars (control cells) show >90% of NCI H292 and MCF7 cancer cells assemble a bipolar spindle at mitosis. Following Cdk-1 inhibition with 10 μM RO3306/10 μM verapamil, both cancer cell lines show ~ 50% drop in bipolar spindle assembly. Middle graph: Centrosome amplification in NCI H292 and MCF7 cells is low in control cells (blue bars) but rises 30–40% in both cancer lines following Cdk-1 inhibition by RO3306i treatment (red bars). Lower graph: Chromosome alignment at the metaphase spindle is significantly lower (40–80%) in both cancer cell lines following RO3306i (red bars) compared to control cells (blue bars).

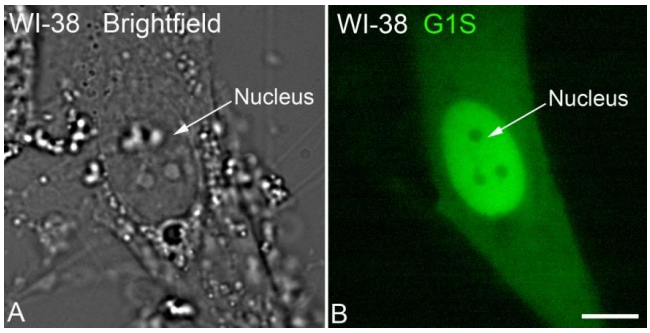

Figure 13. G1S cell cycle indicator probe in live WI-38 lung fibroblasts. A: Bright field image of an interphase WI-38 cell with prominent nucleus (arrow).
B: Presence of G1S probe in nucleus indicates that this cell is at the G1 stage. Bar= 5 μm.

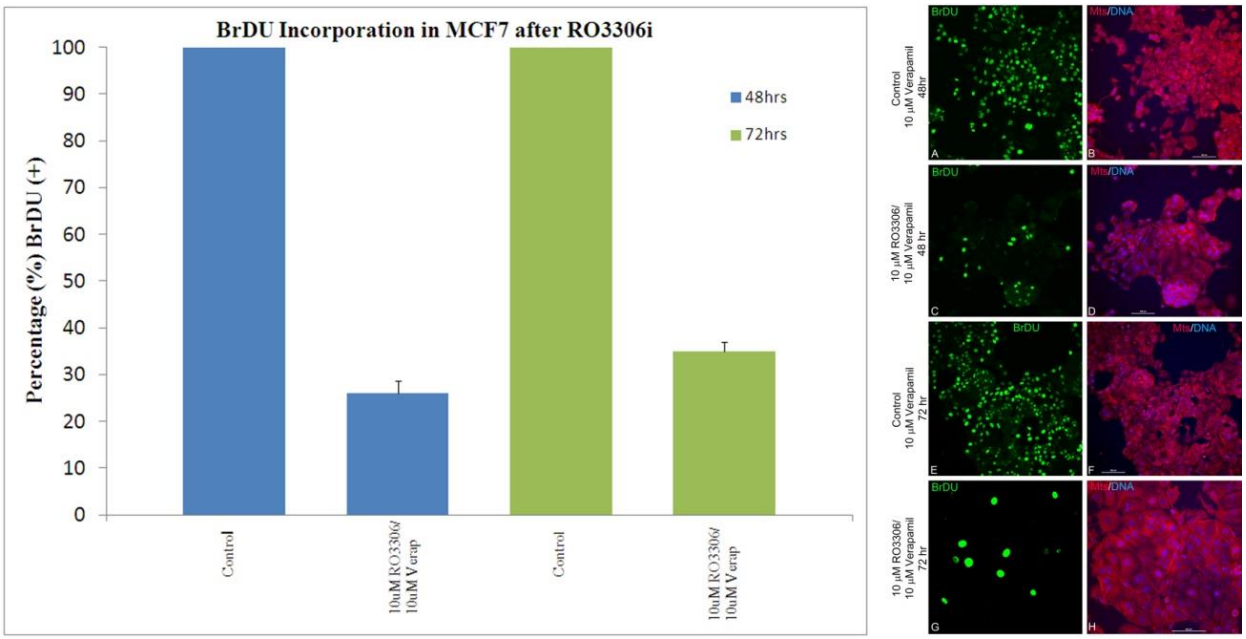

Figure 14. Effects of Cdk-1 inhibition with 10 μM RO3306/10 μM verapamil for 72 hrs on DNA replication as detected by BrDU incorporation in MCF7 breast cancer cells. Graph: Percentage of BrDU-positive MCF7 cells in control (10 μM verapamil) and 10 μMRO3306/10 μM verapamil-treated cells at 48 hrs (blue bar) and 72 hrs (green bars). BrDU labeling compound was added during the last 16 hrs of culture prior to fixation and detection with fluorescent anti-BrDU antibody. At both time points, <70% of MCF7 cancer cells treated with the RO3306i completed DNA replication compared to control cells. Right panels: Images of BrDU-positive cells in control (A and E; green) and RO3306i-treated MCF7 cells (C and G; green) at 48 and 72 hrs post Cdk-1 inhibition, respectively. B, D, F, and H: corresponding microtubule (red) and DNA (blue) images. Fewer BrDU (+) cells are observed after Cdk-1 inhibition with RO3306i. Bars= 100 nm.

Table 1. Summary of TLVM Experiments on GFP-Centrin Expressing Cancer Cells

Cancer cell type	Number of TLVM trials (total cells)	Cancer cell treatment[1]	Number of cells imaged at:		Number of developing from interphase → mitosis (%)	Number of mitotics which divided (%)
			Interphase	Mitosis		
NCI H292	5 (37)	Control	9	10	1/9 (11)	10/10 (100)
		RO3306i	12	6	1/12 (8)	3/6 (50)
MCF7	9 (42)	Control	1	8	0/1 (0)	5/8 (63)
		RO3306i	15	18	1/15 (7)	3/18 (17)

[1]Control: 10 μM verapamil or Tariquidar anti-MDR compound only; RO3306i: inhibitor of Cdk-1 (10–20 μM).

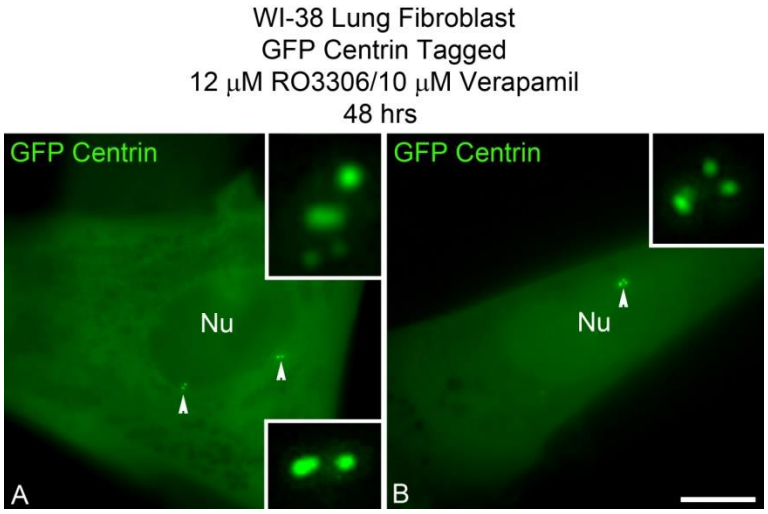

Figure 15. Interphase GFP-centrin-tagged WI-38 lung fibroblasts treated 48 hrs with 12 μM RO3306/10 μM verapamil. A: cell with eight GFP-centrin-expressing centrioles (green, arrowheads; inset: centriole details) after RO3306i. Centrioles separated unequally along the nuclear surface (Nu). B: duplicated GFP-centrin-expressing centrioles (green, arrowhead; inset: centriole details) adjacent to nuclear surface (Nu) after RO3306i. Bar=5 um.

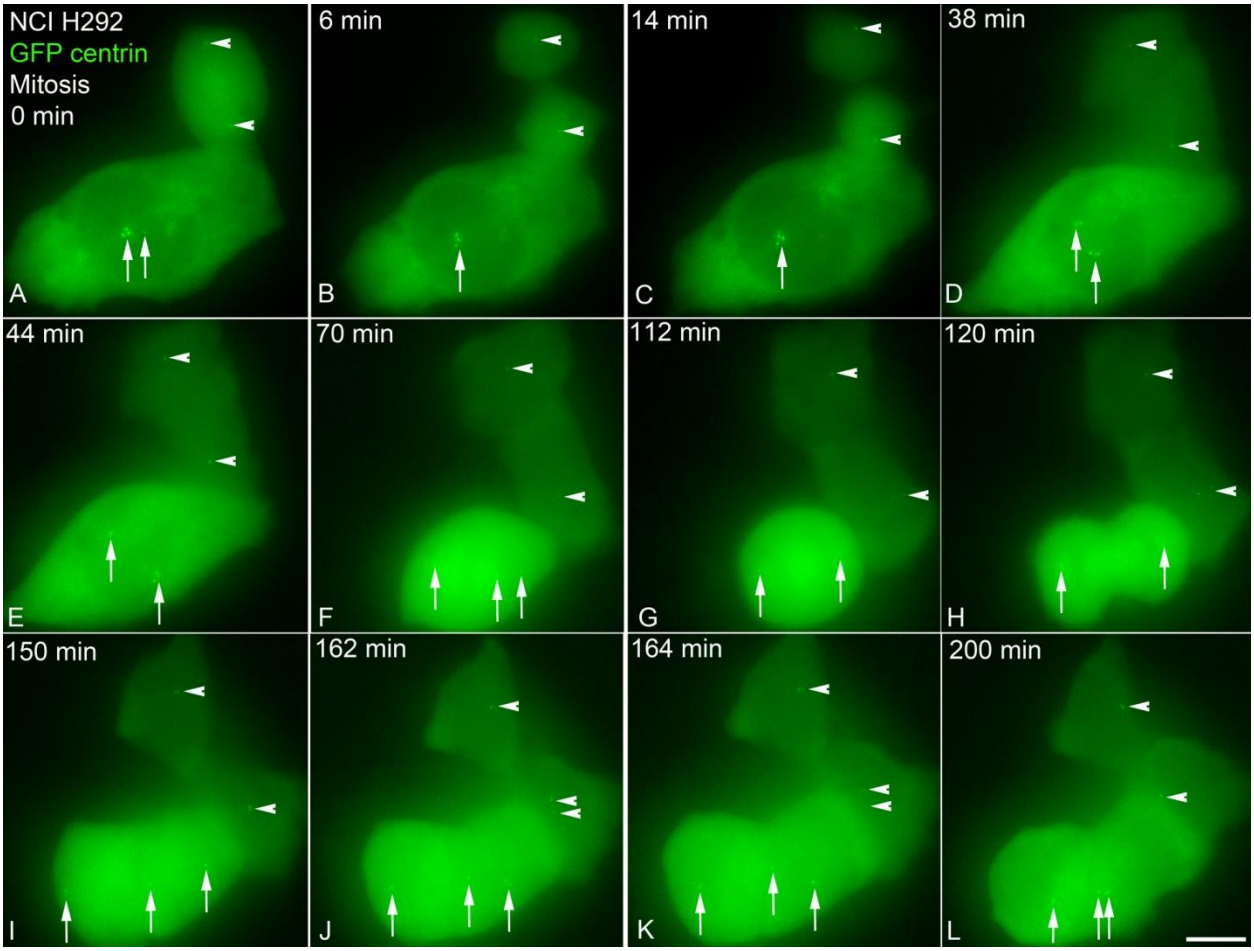

Figure 16. TLVM of two GFP centrin-tagged NCI H292 cells after 10 μM RO3306 for 48hrs. Imaging began 2 hrs post-RO3306i recovery. A: Telophase with normal centrioles at the spindle poles is visible in the upper cell (green, arrowheads) while interphase with multiple adjacent centrioles is shown in the lower cell (green, arrows). B–E: Upper cell completes cell division and divides normally, with single centrioles visible at each pole (green, arrowheads). The lower cell begins to separate the duplicated centrioles along the nuclear surface (green, arrows).
F–L: Upper divided cell shows centrioles in each daughter cell (green, arrowheads), with an indication of multiple centrioles in the lower daughter cell visible in panels J and K (green, double arrowheads). The lower cell undergoes nuclear envelope breakdown in panel F, assembling a bipolar spindle, but with atypical centriole numbers at the poles (green, arrows). In panel G, the lower mitotic cell has undergone chromosome segregation, and the centrioles appear to be "clustered" at both poles as the cell undergoes cell division (G-H: green, arrows). During the latter stages of cytokinesis in panels I–L, at least three distinct centrioles are visible (green, arrows), which show rapid movement in the cytoplasm as the cell completes the division process. Z-series imaging at 2 min intervals for 200 min. Time in min: upper left. Bar= 5 μm.

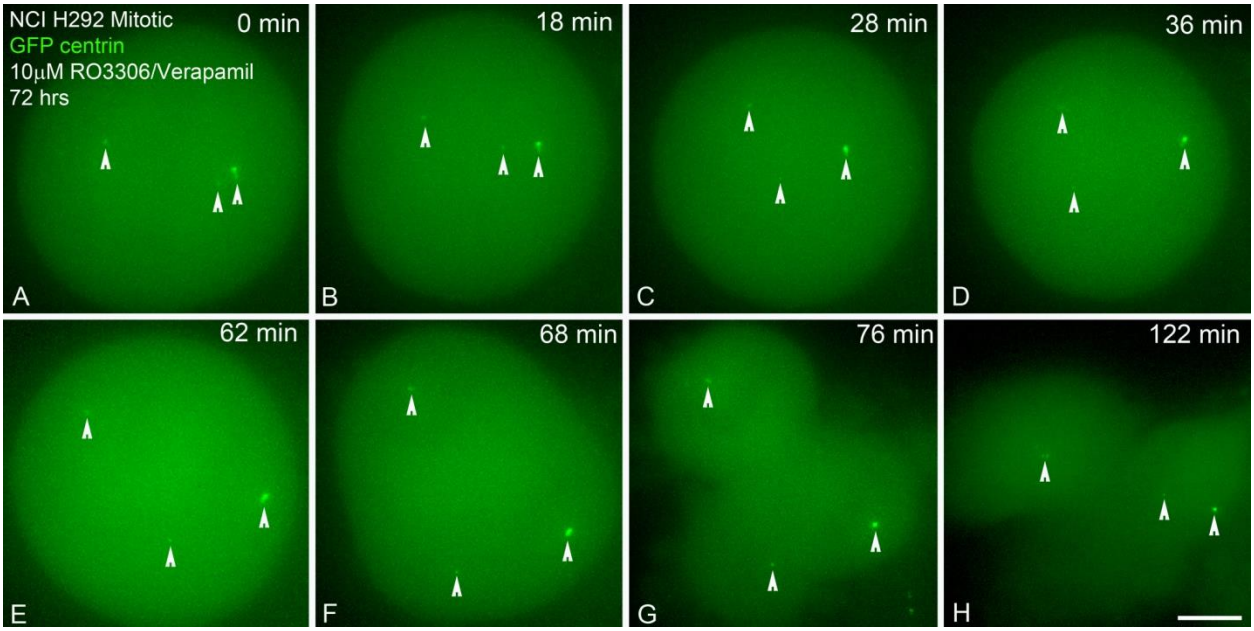

Figure 17. Time-lapse video of GFP-centrin-expressing NCI H292 cancer cell following rescue from simultaneous 72-hr treatment with 10μM RO3306 Cdk1 inhibitor and 10μM verapamil. A: Time 0 following a 2.5-hr recovery from drug treatment, showing mitotic cell with more than four observed centrioles, some tightly paired (green; arrowheads). B–E: One centriole pair migrates away from the brightest centriole cluster, forming a third spindle pole (green; lower arrowheads). F–G: The cell appears to divide 1→3 at the end of cell division.H: Lower two daughter blastomeres fuse together, creating the appearance of a single divided cell, but with abnormal centrioles apparent by GFP centrin (green; arrowheads). Time: minutes post imaging. Z-series imaging at 2 min intervals for 122 minutes: Bar= 5 μm.

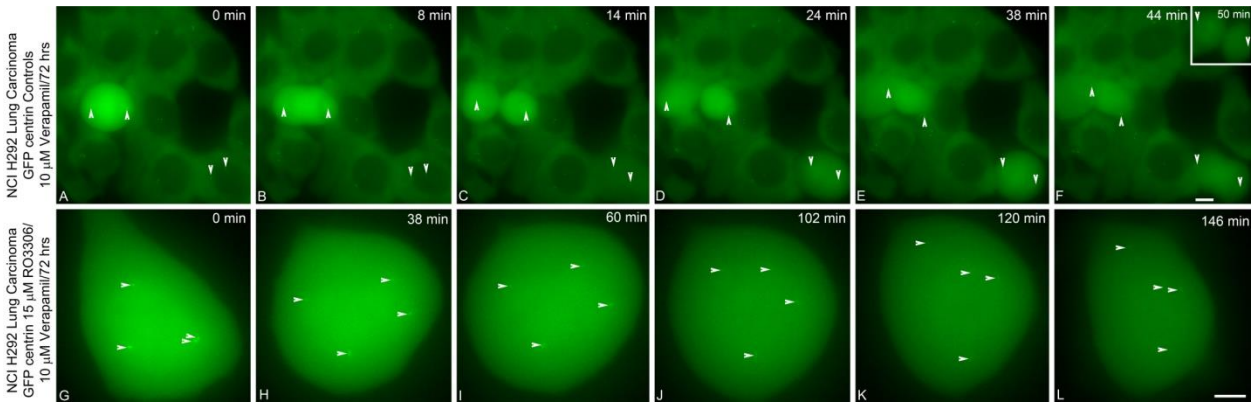

Figure 18. Selected TLVM images of mitotic progression in GFP-centrin-tagged NCI H292 lung carcinoma cells after 10 μM verapamil (controls) or 15 μM RO3306i for 72 hrs. A–F: Control cells. Middle cell in panels A–F depicts normal cell division beginning at anaphase (A: 0 min; arrowheads: GFP-centrin-tagged centrioles) and ending with normal cell division after 44 minutes (F: arrowheads; GFP centrin-tagged centrioles). Lower right cell in panels A–F shows progression from late interphase (A: 0 min; arrowheads; centrioles) through normal cell division (F: inset; arrowheads, centrioles) by 50 min. G–L: Tetrapolar cell with four GFP centrin-tagged centrioles (arrowheads) following RO3306i. Imaging 24 hrs post drug recovery. Neither centriole clustering nor cell division was observed after 146 min (L). Bars=5 μm.

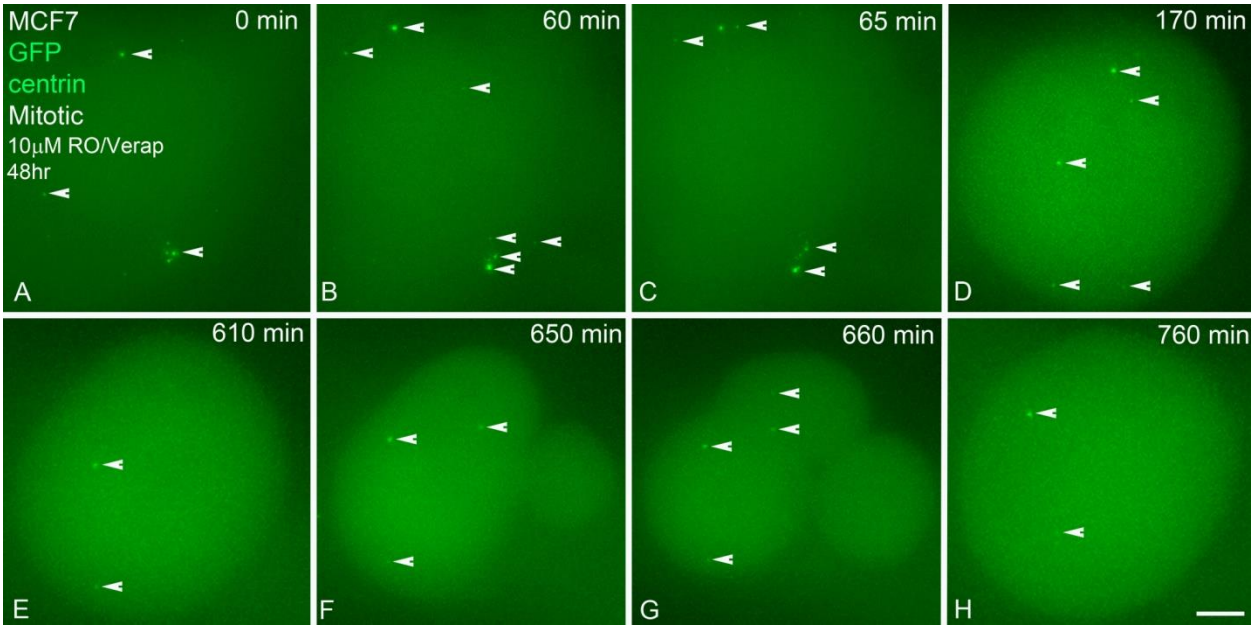

Figure 19. TLVM of a mitotic MCF7 breast cancer cell after treatment with 10 μM RO3306 Cdk-1 inhibitor/10 μM verapamil for 48 hrs. Imaging at 15 min post RO3306i recovery. A: Mitotic prometaphase stage, showing hyperamplification of centrioles by GFP centrin (green, arrowheads). A minimum of eight centrioles could be identified in this cell (B: green, arrowheads). C–D: As the MCF7 cell rounds up for mitosis, GFP centrin-tagged centrioles appear to disperse throughout the cytoplasm without defining a bipolar spindle at the cell center (C-D: green, arrowheads). E: At 610 min post imaging, the cell is still rounded, and detection of the GFP centrin-tagged centrioles is less extensive (green; arrowheads). F–H: At 650 min, the cell attempts an unequal cell division with GFP centrin-tagged centrioles still widely dispersed in the cytoplasm (F and G: green, arrowheads). By 760 min post imaging, cytokinesis fails to complete and the cell begins to flatten onto the coverslip surface as a few centrioles migrate around the cytoplasm (H: green, arrowheads). Z-series imaging at 5 min intervals for over 12 hrs. Bar= 5 μm.

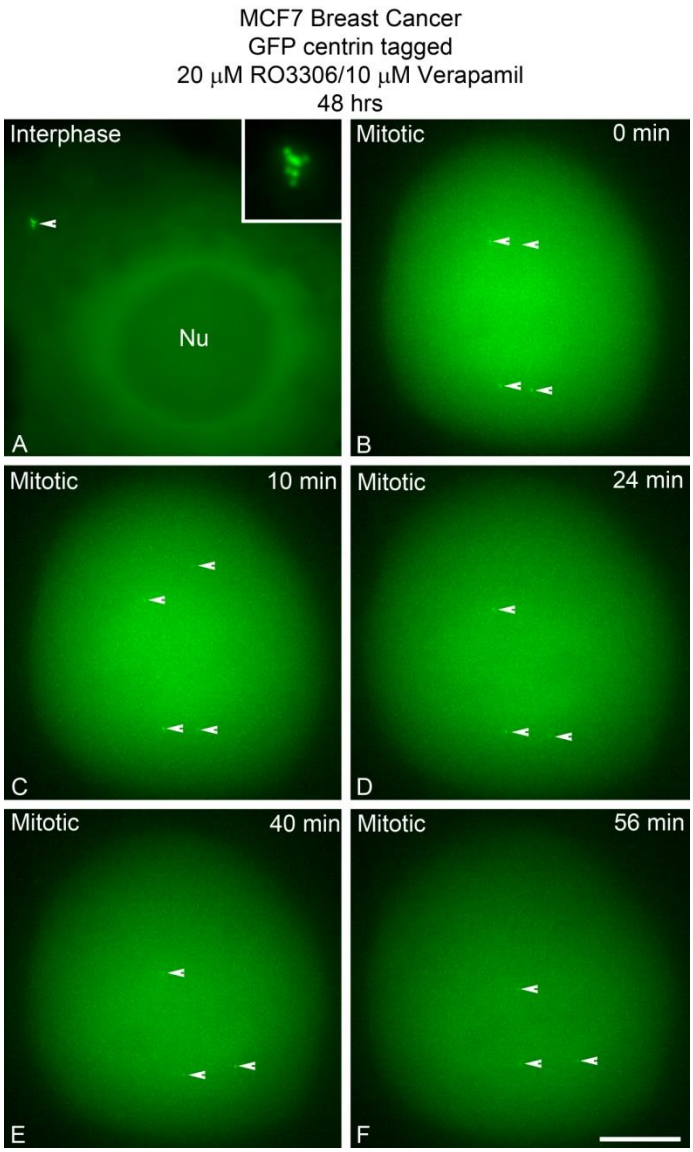

Figure 20. TLVM of GFP centrin-tagged MCF7 breast cancer cells following 20 μM RO3306/10 μM verapamil for 48 hrs. Imaging at 24 hrs post RO3306i recovery.
A: MCF7 interphase cell depicting centriole hyperamplification (green, arrowheads; inset: centriole details; Nu: nucleus) after RO3306i.
B–F: Panels from a TLVM movie of a mitotic cell with four distinct centrioles (B: green, arrowheads). By 56 min post imaging, the metaphase spindle collapses without cytokinesis onset (C–F: green, arrowheads, centrioles). Three of four centrioles remain with the collapsing spindle, and one centriole displaces toward the cytoplasm. Bar=5 μm.

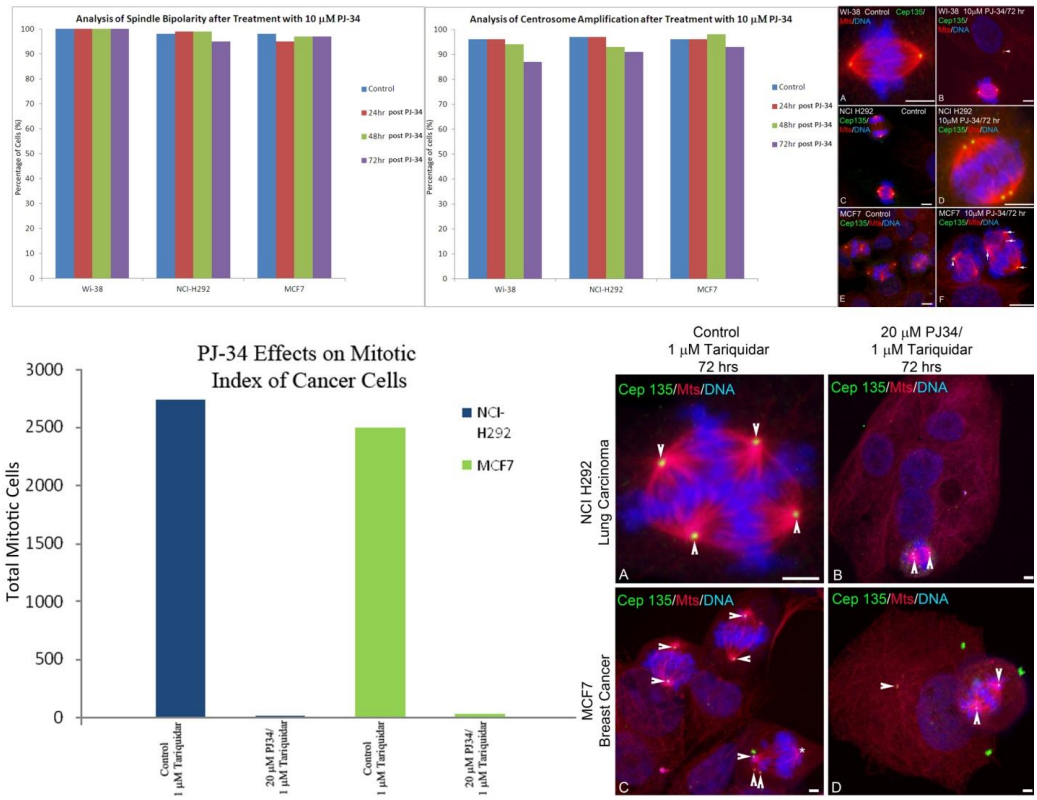

Figure 21. The PARP inhibitor PJ-34 did not block cell cycle progression but greatly reduced the mitotic index in NCI H292 and MCF7 cancer cells. Upper graphs: Treatment of WI-38, NCI H292, and MCF7, for 24 (red bars), 48 (green bars), or 72 (purple bars) hrs, with 10 μM PJ-34 did not impact bipolar spindle assembly or centrosome amplification significantly when compared to control cells (blue bars). Upper right panels: Selected representative images of mitotic control (A, C, E) and 10 μM PJ-34 (B, D, and F) -treated WI-38 (A–B), NCI H292 (C–D), and MCF7 (E–F) cells 72 hrs after PARP inhibition. Most mitotic cells demonstrated normal bipolar spindles (red, microtubules) with correct centrioles at the poles (green) and aligned chromosomes (blue, DNA), although some MCF7 cells occasionally displayed multipolar spindles (red, microtubules) with amplified centrosomes (green, arrows) and misaligned chromosomes (blue, DNA). Lower left graph: Total counts of mitotic cells observed in control (1 μM tariquidar) and 20 μM PJ-34/1 μM tariquidar-treated cancer cells. Total mitotic cell counts dropped 136- fold in NCI H292 lung carcinoma cells and 86-fold in MCF7 breast cancer cells. Lower right panels: Representative images from control and PJ-34-treated cancer cells. Control metaphase NCI H292 (A: blue, DNA) and MCF7 cells (C: blue, DNA) displayed many tetrapolar spindles and amplified centrosomes (A, C: red, microtubules; green; centrosomes, arrowheads). Conversely, exposure to PJ-34 for 72 hrs in NCI H292 (B: blue, DNA) and MCF7 cells (D: blue, DNA) greatly reduced, but did not eliminate, mitotic cells, although no multipolar spindles or amplified centrosome numbers were observed in PJ-34-exposed cells (B and D: red, microtubules; green, centrosomes, arrowheads). All ICC images are tripled labeled for Cep135 centrioles (green), microtubules (red), and DNA (blue). Bars=5 μm.

18. Extent of Clinical Activities Initiated and Completed. Items 18(A) and 18(B) should be completed for all research projects. If the project was restricted to secondary analysis of clinical data or data analysis of clinical research, then responses to 18(A) and 18(B) should be "No."

18(A) Did you initiate a study that involved the testing of treatment, prevention or diagnostic procedures on human subjects?

_____Yes
___X__No

18(B) Did you complete a study that involved the testing of treatment, prevention or diagnostic procedures on human subjects?

_____Yes
___X__No

If "Yes" to either 18(A) or 18(B), items 18(C) – (F) must also be completed. (Do NOT complete 18(C-F) if 18(A) and 18(B) are both "No.")

18(C) How many hospital and health care professionals were involved in the research project?

_____Number of hospital and health care professionals involved in the research project

18(D) How many subjects were included in the study compared to targeted goals?

_____Number of subjects originally targeted to be included in the study
_____Number of subjects enrolled in the study

Note: Studies that fall dramatically short on recruitment are encouraged to provide the details of their recruitment efforts in Item 17, Progress in Achieving Research Goals, Objectives and Aims. For example, the number of eligible subjects approached, the number that refused to participate and the reasons for refusal. Without this information it is difficult to discern whether eligibility criteria were too restrictive or the study simply did not appeal to subjects.

18(E) How many subjects were enrolled in the study by gender, ethnicity and race?

Gender:
_____Males
_____Females
_____Unknown

Ethnicity:
_____Latinos or Hispanics
_____Not Latinos or Hispanics
_____Unknown

Race:
_____American Indian or Alaska Native
_____Asian
_____Blacks or African American
_____Native Hawaiian or Other Pacific Islander
_____White
_____Other, specify:_____
_____Unknown

18(F) Where was the research study conducted? (List the county where the research study was conducted. If the treatment, prevention and diagnostic tests were offered in more than one county, list all of the counties where the research study was conducted.)

19. Human Embryonic Stem Cell Research. Item 19(A) should be completed for all research projects. If the research project involved human embryonic stem cells, items 19(B) and 19(C) must also be completed.

19(A) Did this project involve, in any capacity, human embryonic stem cells?
_____Yes
_X___ No

19(B) Were these stem cell lines NIH-approved lines that were derived outside of Pennsylvania?
_____Yes
_____ No

19(C) Please describe how this project involved human embryonic stem cells:

20. Articles Submitted to Peer-Reviewed Publications.

20(A) Identify all publications that resulted from the research performed during the funding period and that have been submitted to peer-reviewed publications. Do not list journal abstracts or presentations at professional meetings; abstract and meeting presentations should be listed at the end of item 17. **Include only those publications that acknowledge the Pennsylvania Department of Health as a funding source** (as required in the grant agreement). List the title of the journal article, the authors, the name of the peer-reviewed publication, the month and year when it was submitted, and the status of publication (submitted for publication, accepted for publication or published.). Submit an electronic copy of each publication or paper submitted for publication, listed in the table, in a PDF version 5.0.5 (or greater) format, 1,200 dpi. Filenames for each publication should include the number of the research project, the last name of the PI, the number of the publication and an abbreviated research project title. For example, if you submit two publications for PI Smith for the "Cognition and MRI in Older Adults" research project (Project 1), and two

publications for PI Zhang for the "Lung Cancer" research project (Project 3), the filenames should be:

Project 1 – Smith – Publication 1 – Cognition and MRI
Project 1 – Smith – Publication 2 – Cognition and MRI
Project 3 – Zhang – Publication 1 – Lung Cancer
Project 3 – Zhang – Publication 2 – Lung Cancer

If the publication is not available electronically, provide 5 paper copies of the publication.

Note: The grant agreement requires that recipients acknowledge the Pennsylvania Department of Health funding in all publications. Please ensure that all publications listed acknowledge the Department of Health funding. If a publication does not acknowledge the funding from the Commonwealth, do not list the publication.

Title of Journal Article:	Authors:	Name of Peer-reviewed Publication:	Month and Year Submitted:	Publication Status (check appropriate box below):
1. None				☐Submitted ☐Accepted ☐Published

20(B) Based on this project, are you planning to submit articles to peer-reviewed publications in the future?

Yes___X_____ No_____

If yes, please describe your plans:

The discoveries made here are being analyzed and confirmed. Once that work is completed, then they will be prepared for publication in a prominent cell and cancer biology journal.

21. Changes in Outcome, Impact and Effectiveness Attributable to the Research Project. Describe the outcome, impact, and effectiveness of the research project by summarizing its impact on the incidence of disease, death from disease, stage of disease at time of diagnosis, or other relevant measures of outcome, impact or effectiveness of the research project. If there were no changes, insert "None"; do not use "Not applicable." Responses must be single-spaced below, and no smaller than 12-point type. DO NOT DELETE THESE INSTRUCTIONS. There is no limit to the length of your response.

None

22. Major Discoveries, New Drugs, and New Approaches for Prevention Diagnosis and Treatment. Describe major discoveries, new drugs, and new approaches for prevention, diagnosis and treatment that are attributable to the completed research project. If there were

no major discoveries, drugs or approaches, insert "None"; do not use "Not applicable." Responses must be single-spaced below, and no smaller than 12-point type. DO NOT DELETE THESE INSTRUCTIONS. There is no limit to the length of your response.

None

23. Inventions, Patents and Commercial Development Opportunities.

23(A) Were any inventions, which may be patentable or otherwise protectable under Title 35 of the United States Code, conceived or first actually reduced to practice in the performance of work under this health research grant? Yes_____ No___X_____

If "Yes" to 23(A), complete items a – g below for each invention. (Do NOT complete items a - g if 23(A) is "No.")

a. Title of Invention:

b. Name of Inventor(s):

c. Technical Description of Invention (describe nature, purpose, operation and physical, chemical, biological or electrical characteristics of the invention):

d. Was a patent filed for the invention conceived or first actually reduced to practice in the performance of work under this health research grant?
Yes_____ No____

If yes, indicate date patent was filed:

e. Was a patent issued for the invention conceived or first actually reduced to practice in the performance of work under this health research grant?
Yes_____ No____
If yes, indicate number of patent, title and date issued:
Patent number:
Title of patent:
Date issued:

f. Were any licenses granted for the patent obtained as a result of work performed under this health research grant? Yes_____ No____

If yes, how many licenses were granted?_____

g. Were any commercial development activities taken to develop the invention into a commercial product or service for manufacture or sale? Yes___ No____

If yes, describe the commercial development activities:

23(B) Based on the results of this project, are you planning to file for any licenses or patents, or undertake any commercial development opportunities in the future?

Yes_____ No____X_____

If yes, please describe your plans:

24. Key Investigator Qualifications. Briefly describe the education, research interests and experience and professional commitments of the Principal Investigator and all other key investigators. In place of narrative you may insert the NIH biosketch form here; however, please limit each biosketch to 1-2 pages. *For Nonformula grants only – include information for only those key investigators whose biosketches were not included in the original grant application.*

BIOGRAPHICAL SKETCH

NAME	POSITION TITLE
Calvin Simerly, PhD	Research Associate Professor

EDUCATION/TRAINING

INSTITUTION AND LOCATION	DEGREE *(if applicable)*	YEAR(s)	FIELD OF STUDY
Pensacola Junior College, Pensacola, Florida	A.A.	1974-1976	Biology
Florida State University Tallahassee, Florida	B.S.	1976-1979	Biological Science
University of Wisconsin Madison, Wisconsin	Ph.D.	1995-1998	Endocrinology-Reproductive Sciences

A. Positions and Honors

Positions

1979-1983 Department of Biological Sciences, Laboratory Technologist
Florida State University, Tallahassee, Florida

1984-1986 Department of Biological Sciences Biological Scientist
Florida State University, Tallahassee, Florida

1986-1989 Department of Zoology, Senior Research Specialist
University of Wisconsin, Madison, Wisconsin

1990-1995 Department of Zoology, Associate Researcher
University of Wisconsin, Madison, Wisconsin

1995-1997 Department of Zoology, Assistant Scientist
University of Wisconsin, Madison, Wisconsin

1997-1998 Division of Reproductive Sciences, Staff Scientist I
Oregon Regional Primate Research Center Beaverton, Oregon

1997-1998 Division of Reproductive Sciences Staff Scientist I
Oregon Regional Primate Research Center Beaverton, Oregon

1998-2001 Division of Reproductive Sciences Staff Scientist II (Assistant Professor Equivalent) Oregon Regional Primate Research Center Beaverton, Oregon

1999-2001 Department of Obstetrics/Gynecology Research Assistant Professor
Oregon Health & Science University Portland, Oregon

2001-2008 Department of Obstetrics/Gynecology & Reproductive Sciences,
Research Associate Professor, University of Pittsburgh
Pittsburgh, Pennsylvania

2008-Present Department of Obstetrics/Gynecology & Reproductive Sciences
Research Associate Professor, University of Pittsburgh
Pittsburgh, Pennsylvania

B. Selected Peer-Reviewed Publications

1. Simerly C, McFarland D, Castro C, Lin CC, Redinger C, Jacoby E, Mich-Basso J, Orwig K, Mills P, Ahrens E, Navara C, Schatten G. Interspecies chimera between primate embryonic stem cells and mouse embryos: monkey ESCs engraft into mouse embryos, but not post-implantation fetuses. Stem Cell Res. 2011 Jul;7(1):28-40. doi: 10.1016/j.scr.2011.03.002. Epub 2011 Mar 25. PMID: 21543277.

2. Simerly C, Schatten G. Utility of animal models for human embryo culture: nonhuman primates. Methods Mol Biol. 2012;912:39-59. doi: 10.1007/978-1-61779-971-6_4. PMID: 22829368.

3. Easley CA 4th, Phillips BT, McGuire MM, Barringer JM, Valli H, Hermann BP, Simerly CR, Rajkovic A, Miki T, Orwig KE, Schatten GP. Direct differentiation of human pluripotent stem cells into haploid spermatogenic cells. Cell Rep. 2012 Sep 27;2(3):440-6. doi: 10.1016/j.celrep.2012.07.015. Epub 2012 Aug 23. PMID: 22921399.

4. Shi Q, Hodara V, Simerly CR, Schatten GP, Vandeberg JL. Ex vivo reconstitution of arterial endothelium by embryonic stem cell-derived endothelial progenitor cells in baboons. Stem Cells Dev. 2013 Feb 15;22(4):631-42. doi: 10.1089/scd.2012.0313. Epub 2012 Oct 10. PMID: 22931470; PMCID: PMC3564485.

5. Shi Q, Schatten G, Hodara V, Simerly C, Vandeberg JL. Endothelial reconstitution by CD34+ progenitors derived from baboon embryonic stem cells. J Cell Mol Med. 2013 Jan 10. doi: 10.1111/jcmm.12002. [Epub ahead of print] PMID: 23301772.

C. RESEARCH SUPPORT

1R25CA163168-01 (Schatten, G.)
Frontiers in Stem Cells in Cancer; 9/26/11–8/31/16
NIH/NCI

1T15 HD072833 (Schatten, G.P.)
Rehabilitative and Regenerative Medicine for Minority Health & Health Disparities; 9/10/12 – 8/31/15
NIH/NICHD

R25 AG043365 (Schatten, G.P)
Frontiers in Aging and Regenerative Medicine; 9/30/12-8/31/17
NIH/NIA

BIOGRAPHICAL SKETCH

NAME	POSITION TITLE
Schatten, Gerald P. PhD	Professor, Obstetrics and gynecology and reproductive sciences

INSTITUTION AND LOCATION	DEGREE *(if applicable)*	YEAR(s)	FIELD OF STUDY
University of California, Berkeley	A.B.	1971	Zoology
University of California, Berkeley	Ph.D.	1975	Cell Biology
Rockefeller Foundation Fellowship	Postdoc	1976	Reprod Biology
German Cancer Research Center, Heidelberg	Postdoc	1976	Cancer Biology
Rockefeller Foundation Fellowship	Postdoc	1977	Reprod Biology

A. Position and Honors

1975	Instructor, Department of Zoology, Univ. of California, Berkeley.
1976, 1977	Rockefeller Foundation Postdoctoral Fellowship.
1977, 1984	Guest Researcher, German Cancer Research Center, Heidelberg.
1977-1986	Assistant (1977-81), Assoc (1981-85), Prof (1986), Molecular Biophysics; Florida State Univ.
1981-1986	Research Career Development Award, National Institutes of Health.
1985, 1986	Instructor in Embryology, Marine Biological Laboratory, Woods Hole.
1986-1997	Professor of Zoology, Molecular Biology & Ob/Gyn, University of Wisconsin
1986-1992	Director, Integrated Microscopy Resource, University of Wisconsin.
1987-1997	Director, Gamete & Embryo Biology NIH Training Program Core Scientist, Wisconsin Regional Primate Research Center
1997-2001	Endowed Professor of OB/GYN and Cell/Developmental Biology, Oregon Health Sciences University; and Senior Scientist, Oregon Regional Primate Research Center
1998-2001	Founding Course Director, "Frontiers in Reproduction," MBL, Woods Hole
1997-2008	NIH MERIT Award
2001-Pres.	Deputy Director Magee Womens Research Institute, Professor and Vice Chair, Ob/Gyn and Reproductive Sciences, Professor of Cell Biology-Physiology, & of Bioengineering, University of Pittsburgh School of Medicine

Honors (Selected)

2006-2010	Council Member; National Institute of Aging; Working Group on Program (2007-2010)
2007-pres.	Board of Trustee, International Society for In Vitro Fertilization
2010	Elected President: ASRM Special Interest Group on **Regenerative Medicin**
2010	Elected President; UNESCO's International Cell Research Organization (ICRO)
2011	Shield of Honor in Reproductive Medicine, Awarded by Jordanian Society c Fertility and Genetics, presented by H.R.H. Princess Basma; Amman

B. Selected Peer-reviewed Publications (Selected from > 270 peer-reviewed publications)

1. Simerly C, Schatten G. Utility of animal models for human embryo culture: nonhuman primates. Methods Mol Biol. 2012;912:39-59. doi: 10.1007/978-1-61779-971-6_4. PubMed PMID: 22829368.
2. Hermann BP, Sukhwani M, Winkler F, Pascarella JN, Peters KA, Sheng Y, Valli H, Rodriguez M, Ezzelarab M, Dargo G, Peterson K, Masterson K, Ramsey C, Ward T, Lienesch M, Volk A, Cooper DK, Thomson AW, Kiss JE, Penedo MC, Schatten GP, Mitalipov S, Orwig KE. Spermatogonial stem cell transplantation into rhesus testes regenerates spermatogenesis producing functional sperm. Cell Stem Cell. 2012 Nov 2;11(5):715-26. doi: 10.1016/j.stem.2012.07.017. PubMed PMID: 23122294.
3. Schatten G. Cellular promiscuity: explaining cellular fidelity in vivo against unrestrained pluripotency in vitro. EMBO Rep. 2012 Dec 11. doi: 10.1038/embor.2012.198. [Epub ahead of print] PubMed PMID: 23229589.
4. Shi Q, Schatten G, Hodara V, Simerly C, VandeBerg JL. Endothelial Reconstitution by CD34+ Progenitors Derived from Baboon Embryonic Stem Cells. J Cell & Mol Med 2012 (Accepted).
5. Easley CA, Phillips BT, Wu G, Schatten G, Simerly CR. Clinical Implications of Human Spermatogenesis Initiation in Vitro. J Med Sci 2012 (Accepted).

C. Research Support

5 R01 MH087247-02 (Ayyavoo, V.) HIV-1 Associated Dementia: Concomitant Roles
3/9/10–2/28/15
NIH/NIMH

1 R01 HL102177 (Carlisle, D.) Nicotine Dysregulates Lung Differentiation through N-myc
4/1/11 – 3/31/16
NIH/NHLBI

1R25CA163168-01 (Schatten, G.) Frontiers in Stem Cells in Cancer
9/26/11–8/31/16
NIH/NCI

1T15 HD072833 (Schatten, G.P.) Rehabilitative and Regenerative Medicine for Minority Health & Health Disparities
9/10/12 – 8/31/15 NIH/NICHD

R25 AG043365 (Schatten, G.P) Frontiers in Aging and Regenerative Medicine
9/30/12-8/31/17
NIH/NIA